Supplementary figures

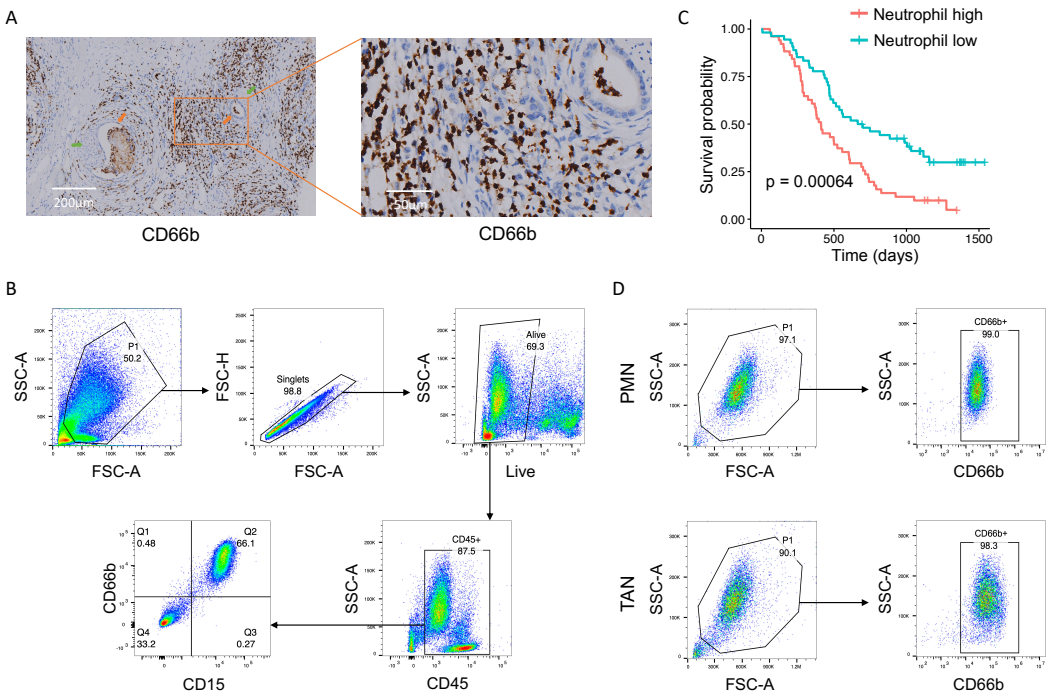

Figure S1. Neutrophils are important infiltrating immune cells in PDAC tumor microenvironment

(A) IHC images of representative PDAC tissues stained for marker genes of neutrophils (CD66b). On the left figure, two duct-like structures formed by malignant cells were highlighted by orange arrows, and peripheral nerves were highlighted by green arrows. Neural invasion of those ductal cells could be observed. (B) Flow cytometry analysis of percentage of $CD15^+$ $CD66b^+$ neutrophils among $CD45^+$ infiltrating immune cells in PDAC tissues. (C) Kaplan-Meier survival curve presenting the overall survival of PDAC patients, divided equally into two groups according to the percentage of infiltrating neutrophils. (D) Typical phenotype of PMNs and TANs isolated from peripheral blood and tumor tissue of PDAC patients using CD66b positive selection. Abbreviations: FSC, forward scatter; SSC, side scatter; PMN, polymorphonuclear leukocytes; TAN, tumor-associated neutrophils.

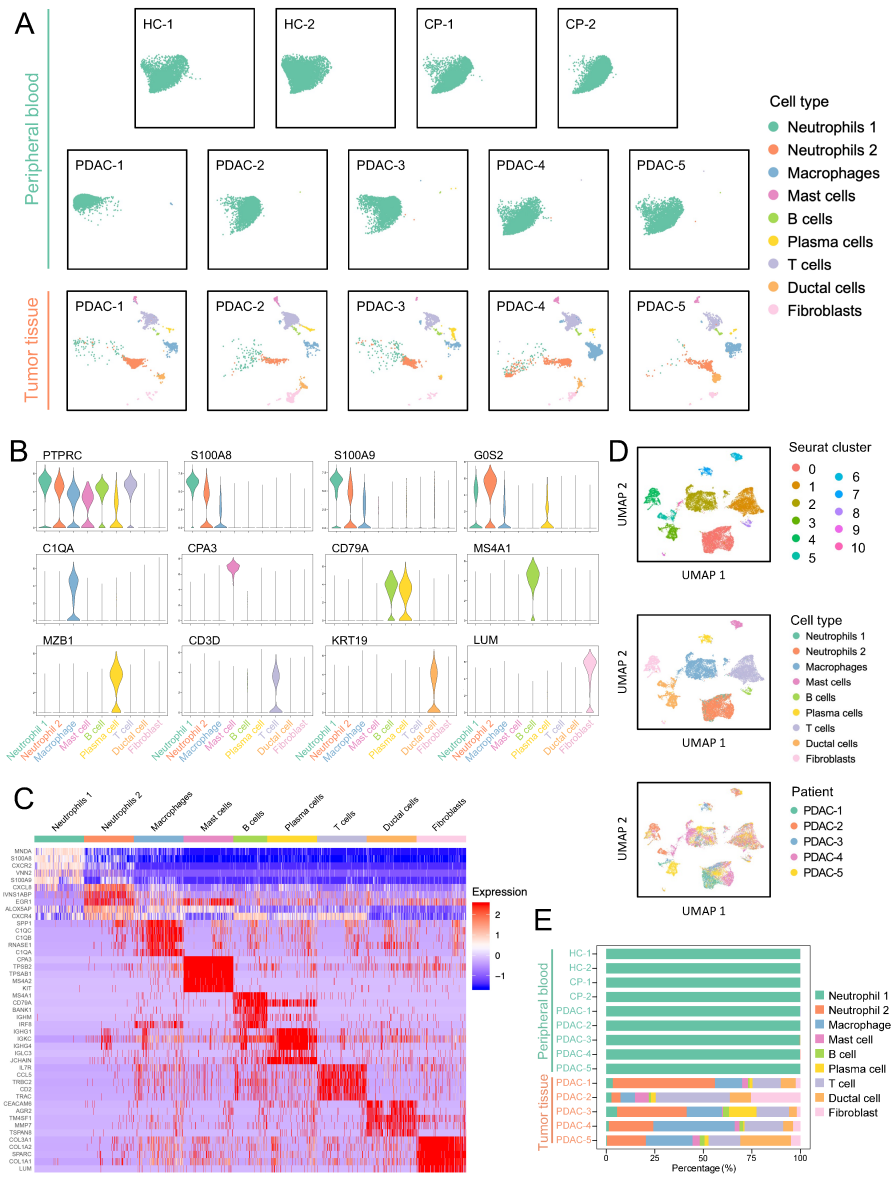

Figure S2. Single-cell atlas from peripheral blood and PDAC tumor tissues, related to Figure 1
(A) UMAP plots of the single cells identified from each sample, with each cell color-coded for cell type. (B) Violin plots showing the expression of representative classical cell type markers. (C) Heatmap showing the expression of top five marker genes in each cell type. (D) Unsupervised clustering of cells from PDAC tissue separately, visualized by UMAP plots, with each cell color-coded for clusters (upper panel), cell type (as annotated in Figure 1B) (middle panel), and the corresponding donor (lower panel). (E) Bar plot depicting the proportions of cell types identified in each sample. Abbreviations: HC, healthy controls; CP, chronic pancreatitis; PDAC, pancreatic ductal adenocarcinoma; UMAP, uniform manifold approximation and projection.

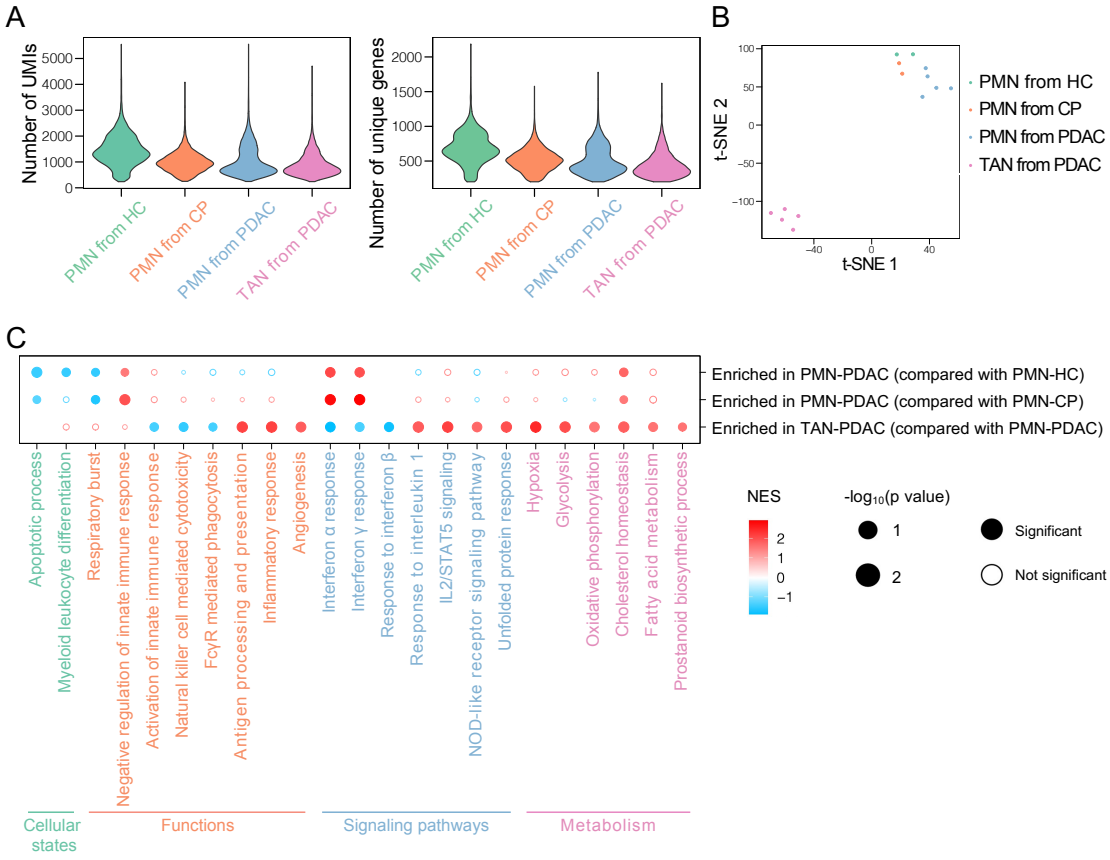

Figure S3. Comparison of the expression profiles of neutrophils from different sources
(A) Violin plots summarizing number of UMIs and number of unique genes detected in neutrophils from different sources. (B) Visualization of the expression profiles of neutrophils from each sample by t-distributed stochastic neighbor embedding (t-SNE) dimensionality reduction analysis. (C) Dot plot showing representative enriched HALLMARK/ KEGG/ GO pathways in TANs and PMNs from PDAC patients. Pathway enrichment analysis was performed with gene set enrichment analysis (GSEA). NES and p values were indicated by circle color and size, respectively. Abbreviations: UMI, unique molecular identifier; HC, healthy controls; CP, chronic pancreatitis; PDAC, pancreatic ductal adenocarcinoma; PMN, polymorphonuclear leukocytes; TAN, tumor-associated neutrophils; t-SNE, t-distributed stochastic neighbor embedding; NES, normalized enrichment score.

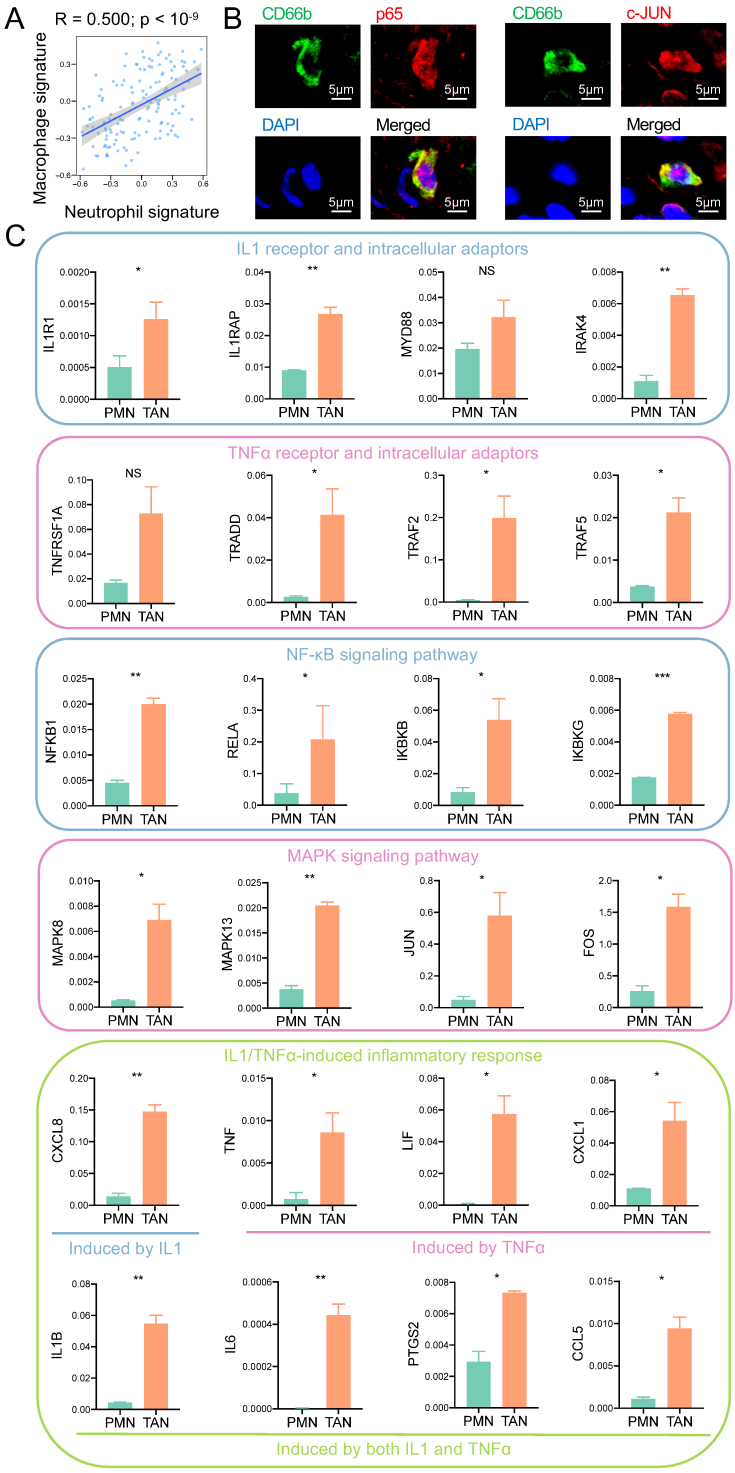

Figure S4. Activation of TNFα and IL1 signaling pathways in TANs, related to Figure 1

(A) Scatterplot showing the expression of neutrophil signatures and macrophage signatures in treatment-naïve PDAC samples from TCGA-PAAD cohort. The association between these variables was assessed by Pearson correlation analysis. (B) Immunofluorescence (IF) staining of CD66b, p65 and c-JUN on PDAC tissue. (C) Comparison of the expression of genes associated with IL1/TNFα signaling between PMNs and TANs isolated from PDAC patients, with qPCR analysis. qPCR data were normalized to fold over β-actin (housekeeping gene), and represented as mean with standard deviation. Abbreviations: PMN, polymorphonuclear leukocytes; TAN, tumor-associated neutrophils.

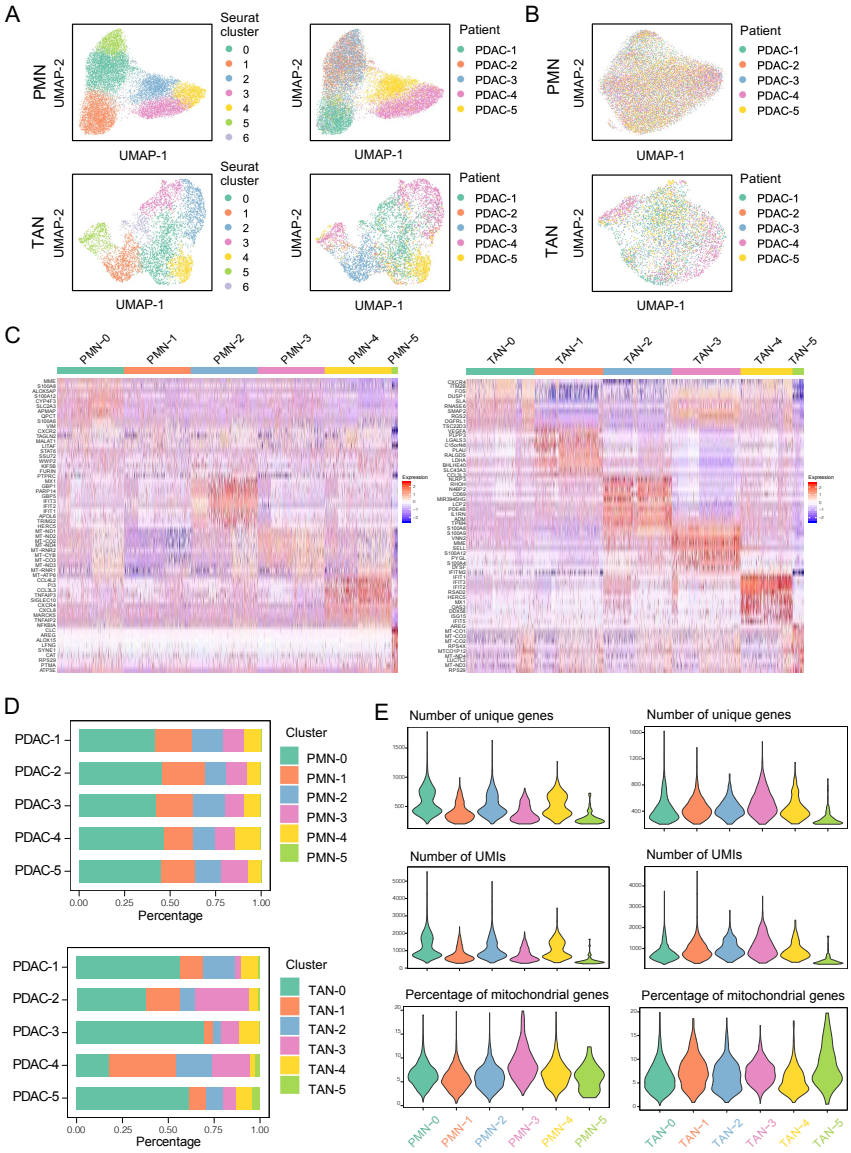

Figure S5. Subclusters of PMNs and TANs from PDAC patients, related to Figure 2

(A) Unsupervised clustering of PMNs and TANs from PDAC patients without batch effect correction, visualized with UMAP plots, with each cell color-coded for clusters (left panel), and the corresponding donor (right panel). (B) UMAP plots of PMNs and TANs from PDAC patients, with each cell color-coded for the corresponding donor, related to Figures 2A-B. (C) Heatmap showing expression of top ten marker genes in each neutrophil cluster. (D) Bar plot depicting the proportions of PMN subclusters and TAN subclusters identified in each sample. (E) Violin plots summarizing number of unique genes, number of UMIs, and percentage of mitochondrial genes in each cell across neutrophil subcluster. Abbreviations: PMN, polymorphonuclear leukocytes; TAN, tumor-associated neutrophils; PDAC, pancreatic ductal adenocarcinoma; UMAP, uniform manifold approximation and projection; UMI, unique molecular identifier.

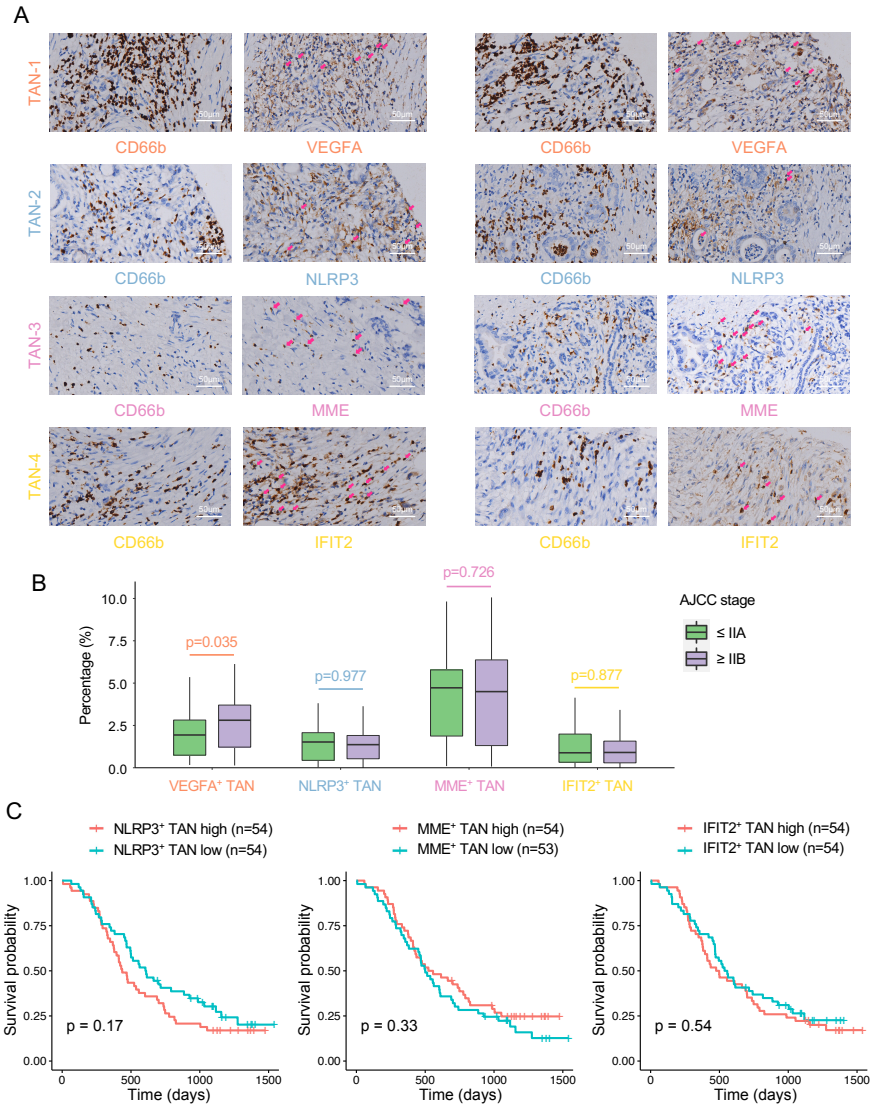

Figure S6. Spatial distribution and clinical relevance of TAN subclusters, related to Figure 3

(A) IHC images of additional representative PDAC tissues stained for marker genes of neutrophils (CD66b) and TAN subclusters (VEGFA for TAN-1, NLRP3 for TAN-2, MME for TAN-3, and IFIT2 for TAN-4) on serial slides. Neutrophils were identified according to CD66b staining on serial slides, and the polynucleated morphology. Pink arrows highlight the neutrophils expressing TAN subcluster markers. (B) Boxplot summarizing the percentages of VEGFA$^+$ TANs, NLRP3$^+$ TANs, MME$^+$ TANs, and IFIT2$^+$ TANs among total cells in PDAC tissues from patients with early-stage disease (AJCC stage ≤IIA) and late-stage disease (AJCC stage ≥IIB). The middle lines represented median values, the boxes represented inter-quartile ranges, and the whiskers extended to the furthest data point within 1.5 times the inter-quartile ranges. Difference between the groups was analyzed by Mann-Whitney U test. (C) Kaplan-Meier survival curve presenting the overall survival of PDAC patients in IHC analysis. The patients were divided equally into two groups according to the percentage of NLRP3$^+$ TANs, MME$^+$ TANs, and IFIT2$^+$ TANs among total cells in PDAC tissues. Abbreviations: TAN, tumor-associated neutrophils.

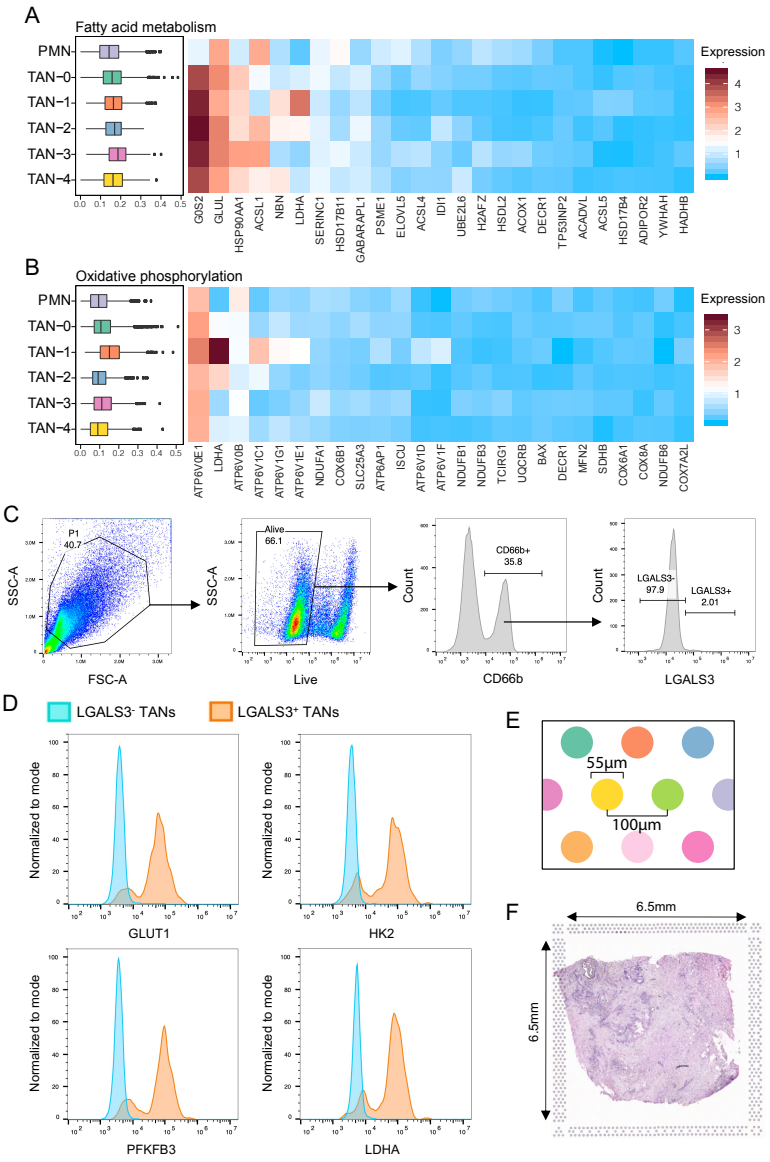

Figure S7. Analysis of metabolic features of TAN subclusters, related to Figure 4

(A-B) Boxplots of expression of hallmark fatty acid metabolism (A) and oxidative phosphorylation (B) signature in each neutrophil subcluster (left panel), and heatmap of average normalized expression of genes in signature (right panel). (C) Gating strategy of flow cytometry analysis of the expression of GLUT1, HK2, PFKFB3 and LDHA in LGALS3^{+} and LGALS3^{-} TANs from PDAC tissues in Figure 4C. (D) Flow cytometry analysis of the expression of GLUT1, HK2, PFKFB3 and LDHA in LGALS3^{+} and LGALS3^{-} TANs from one representative PDAC tissue. (E) Graphical scheme describing the spot size and resolution of spatial transcriptomics. (F) Hematoxylin & Eosin stained PDAC tissue on spatial transcriptomics array. Abbreviations: PMN, polymorphonuclear leukocytes; TAN, tumor-associated neutrophils; FSC, forward scatter; SSC, side scatter.

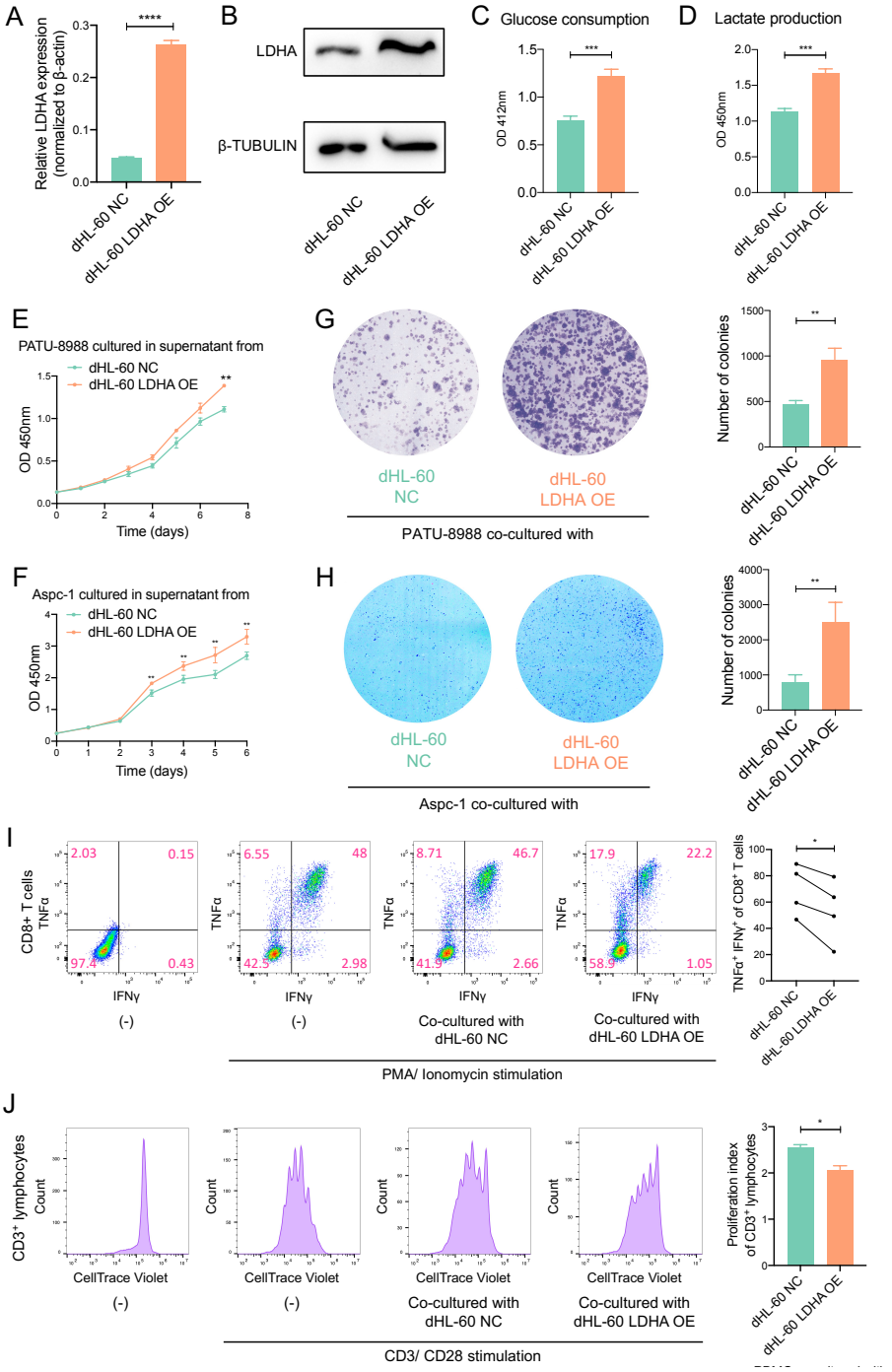

Figure S8. Glycolytic switch enhances pro-tumor functions in TANs

(A-B) Validation of LDHA overexpression in neutrophil-like differentiated HL-60 (dHL-60) cells by qPCR and Western blot. qPCR data were normalized to fold over β-actin (housekeeping gene), and represented as

mean with standard deviation. (C) Bar plot showing glucose consumption in control and LDHA overexpressed dHL-60 cells, assessed by glucose uptake assay kit. Data were represented as mean with standard deviation. (D) Bar plot showing lactate production in control and LDHA overexpressed dHL-60 cells, assessed by L-lactate assay kit. Data were represented as mean with standard deviation. (E-F) PATU-8988 cells (E) and Aspc-1 cells (F) were cultured in the supernatant derived from control and LDHA overexpressed dHL-60 cells, and the proliferation of PATU-8988/ Aspc-1 cells along time course was evaluated by CCK8 assay. (G-H) Colony formation assay, in which control and LDHA overexpressed dHL-60 cells were cultured in upper chambers, and PATU-8988 cells (G) or Aspc-1 cells (H) were cultured in lower chambers. The numbers of colonies were represented as mean with standard deviation. (I) Peripheral blood mononuclear cells (PBMCs) were co-cultured with control and LDHA overexpressed dHL-60 cells for three days, stimulated with PMA/ionomycin, and the percentage of $IFN\gamma^+$ and $TNF\alpha^+$ cells among stimulated $CD8^+$ T cells was analyzed by flow cytometry. Data from 4 different donors were summarized on the right panel. (J) PBMCs were stained with CellTrace Violet, stimulated with anti-human CD3/CD28 for four days in the absence or presence of dHL-60 cells (control or LDHA-overexpressed), and the proliferation of $CD3^+$ lymphocytes was analyzed by flow cytometry. The proliferation index of triplicate cultures were represented as mean with standard deviation. Abbreviations: dHL-60, neutrophil-like differentiated HL-60; NC, negative control; OE, overexpression. * ($p<0.05$); ** ($p<0.01$); *** ($p<0.001$); **** ($p<0.0001$)

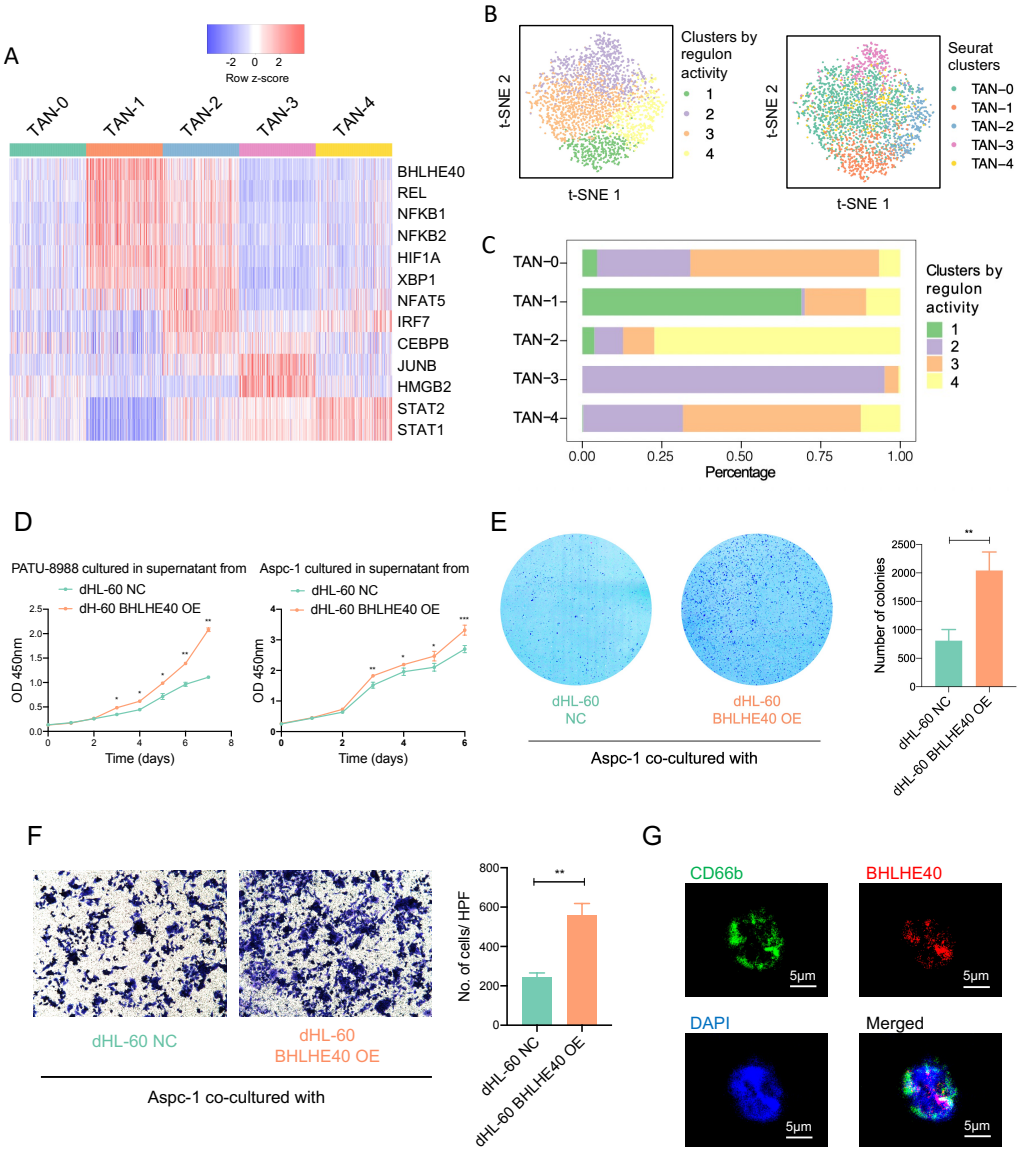

Figure S9. BHLHE40 is a major driver for the pro-tumor phenotype of TAN-1, related to Figures 5-6

(A) Heatmap depicting area under the curve (AUC) scores of representative transcription factors in each TAN subcluster, analyzed using SCENIC. (B) Unsupervised clustering of TANs based on regulon activities, visualized with t-SNE plots, with each cell color-coded for clusters by regulon activity (left panel), and the

original TAN subclusters based on RNA profiles (right panel). (C) Bar plot showing the association between clusters by regulon activity and the original TAN subclusters based on RNA profiles. (D) PATU-8988 cells (left panel) and Aspc-1 cells (right panel) were cultured in the supernatant derived from control and BHLHE40 overexpressed dHL-60 cells, and the proliferation of PATU-8988/ Aspc-1 cells along time course was evaluated by CCK8 assay. (E) Colony formation assay, in which control and BHLHE40 overexpressed dHL-60 cells were cultured in upper chambers, and Aspc-1 cells were cultured in lower chambers. The numbers of colonies were represented as mean with standard deviation. (F) Aspc-1 cells were co-cultured with control and BHLHE40 overexpressed dHL-60 cells for three days, and their migration capacity was assessed by transwell assay. The numbers of migrated cells were represented as mean with standard deviation. (G) Immunofluorescence (IF) staining of CD66b and BHLHE40 on PDAC tissue. Abbreviations: TAN, tumor-associated neutrophils; t-SNE, t-distributed stochastic neighbor embedding; dHL-60, neutrophil-like differentiated HL-60; NC, negative control; OE, overexpression; HPF, high power field. * ($p<0.05$); ** ($p<0.01$); *** ($p<0.001$)